

RESEARCH

Open Access



Mechanical stress facilitates calcium influx and growth of alveolar epithelial cells via activation of the BDKRB1/Ca²⁺/CaMKII/MEK1/ERK axis

Ying Zhang^{1*†}, Qing-dong Zhang^{2†}, Quan Li¹, Zhi-yue Shi¹, Cheng Pan¹, Rong-shuang Yan¹, De-rui Fei¹, Shi-xin Xu¹ and Yang Luo¹

Abstract

Background Mechanical stress and calcium metabolism are associated with lung development and various pulmonary diseases. Our previous research demonstrated that BDKRB1/Ca²⁺ signal transduction may be involved in lung dysplasia resulting from scoliosis and thoracic insufficiency. Therefore, the present study aims to investigate the effects of mechanical stress on the growth and calcium influx in alveolar epithelial cells, as well as the role of BDKRB1/Ca²⁺ signaling in these processes.

Methods Flow cytometry, CCK-8, and EDU staining assay were employed to assess the cycle, calcium influx, activity, and proliferation in RLE-6TN cells subjected to mechanical stresses of varying amplitudes (5%, 10% and 15%). RT-qPCR and western blotting assay were performed to evaluate the effects of mechanical stress on BDKRB1/Ca²⁺/CaMKII/MEK1/ERK signaling in RLE-6TN cells.

Results Mechanical stress at 10% amplitudes effectively enhanced the viability, EDU positive ratio, S-phase percentage, and Ca²⁺ concentration of RLE-6TN cells, while reducing the G1-phase percentage. Conversely, 15% mechanical stress exerted an inhibitory effect on RLE-6TN cell proliferation. Additionally, 10% mechanical stress significantly upregulated the expression of BDKRB1, CaMKII α/δ , p-MEK1 and p-ERK1/2 in RLE-6TN cells. Notably, BDKRB1 knockdown attenuated the 10% mechanical stress-induced increase in both growth and calcium influx in RLE-6TN cells. Moreover, BDKRB1 knockdown blocked the activation of the Ca²⁺/CaMKII/MEK1/ERK pathway induced by 10% mechanical stress.

Conclusion Appropriate levels of mechanical stress contribute to the growth and calcium influx of alveolar epithelial cells by modulating BDKRB1/Ca²⁺/CaMKII/MEK1/ERK signaling.

Keywords Alveolar epithelial cells, Mechanical stress, Calcium, Growth, Bradykinin receptor B1

[†]Ying Zhang and Qing-dong Zhang contributed equally to this study.

*Correspondence:

Ying Zhang

zhangying6@kmmu.edu.cn

Full list of author information is available at the end of the article



Introduction

The lungs are continuously subjected to mechanical forces throughout the respiratory cycle due to the repetitive expansion and contraction occurring during inhalation and exhalation. Mechanical stress modulates cellular behavior and function during development, injury, and repair of lung tissues, particularly in vascular endothelial cells and alveolar epithelial cells, which constitute the vascular and broncho-alveolar networks [1–3]. The extracellular matrix (ECM) serves a critical role in transmitting external physical forces to cells, while also providing structural support and facilitating respiratory function. The influence of mechanical stress on cell-ECM interactions, especially between alveolar epithelial cells and vascular endothelial cells, is pivotal for the establishment and maintenance of mechanical homeostasis. However, non-physiologic mechanical loading can contribute to various pulmonary diseases, including pulmonary fibrosis, acute respiratory distress syndrome (ARDS), ventilation-induced lung injury, and pulmonary hypertension [3–6]. Notably, a variety of intracellular signaling pathways involved in mechanotransduction regulate physiological homeostasis in these lung-associated conditions, including the integrins-FAK-MAPK-NF- κ B, Rho GTPase-YAP/TAZ, and Hippo pathways [7–9]. Therefore, elucidating the molecular mechanisms driven by mechanical stress is essential for improving lung function and promoting vascular and broncho-alveolar network remodeling.

BDKRB1 is located on chromosome 14q32.1-q32.2 and encodes a protein that belongs to the small-molecule G protein-coupled receptor (GPCR) family. These receptors are rapidly upregulated following various types of tissue injury and/or inflammation and are involved in immune responses, neuropathic pain, vasodilation, and tissue repair [10–12]. Our previous study demonstrated that *BDKRB1* expression was reduced in lung tissues from a piglet model of scoliosis combined with thoracic dysplasia-induced pulmonary hypoplasia [13]. Notably, *BDKRB1* expression significantly increased following treatment with a growth-friendly system designed to improve lung tissue development in piglets. Previous research has demonstrated that *BDKRB1* is implicated in the pathogenesis of lung cancer and idiopathic pulmonary fibrosis [14, 15] and also serves as a therapeutic target of sivelestat in the treatment of ARDS [16]. These findings suggest that *BDKRB1* may be responsive to mechanical stress during lung development. Furthermore, *BDKRB1* is recognized as a calcium channel regulator and has been shown to modulate calcium metabolism in glioblastoma cells, osteoblasts, and alveolar macrophages [17–19]. Calcium metabolism itself plays a critical role in the mechanical stress-induced

remodeling of vascular and broncho-alveolar networks [20–22]. Therefore, we hypothesized that mechanical stress may regulate calcium metabolism during lung development through *BDKRB1*-mediated signaling.

In summary, this study employed the FX-5000T Tension System to apply mechanical stress to alveolar epithelial cells, with the aim of investigating its impact on *BDKRB1* expression and elucidating the roles of mechanical stress and *BDKRB1* in regulating calcium metabolism. The goal is to provide new insights into the mechanobiological regulation of vascular and broncho-alveolar network remodeling in lung-related diseases.

Materials and methods

Alveolar epithelial cell culture

RLE-6TN rat alveolar epithelial cells (Catalog No. BNCC337708) were obtained from BNCC (China). Cells were cultured in complete RPMI-1640 medium (Gibco, USA), comprising 89% RPMI-1640, 1% p/s, and 10% FBS. The cells were divided into Con, 10% MS, Lv-NC and Lv-*BDKRB1* groups. Following trypsinization, RLE-6TN cells (2×10^4 cells/well) in the Lv-NC and Lv-*BDKRB1* groups were seeded into 12-well plates. When RLE-6TN cells reached 40%–50% confluency, the medium was replaced with complete medium containing 5 μ g/mL polybrene, excluding penicillin–streptomycin. Cells were transduced with 5 μ L of either control lentivirus or *BDKRB1*-targeting lentivirus (Genomeditech, China) in the Lv-NC and Lv-*BDKRB1* groups, respectively. At approximately 70% cell confluency, cells were subjected to puromycin selection using 5 μ g/mL puromycin (MCE, USA). Knockdown efficiency of *BDKRB1* in RLE-6TN cells was validated using RT-qPCR assay. The short hairpin RNA (shRNA) sequences targeting *BDKRB1* were as follows: TGCTTGAACCCACTGATTAT (#1), ATTCCTTCTACGCTCTGTAA (#2), and GCGCTTAACCATAGCGGAAAT (#3). The corresponding titers of the lentiviral constructs were 5×10^8 TU/mL (#1), 1×10^8 TU/mL (#2), and 1×10^8 TU/mL (#3). RLE-6TN cells from the Con, 10% MS, Lv-NC, and Lv-*BDKRB1* groups were subsequently collected for mechanical stress treatment.

Mechanical stress treatment

Mechanical stress was applied to RLE-6TN cells using the FX-5000T Tension System (Flexcell International, USA), a vacuum-driven apparatus designed to deliver biaxial strain to cultured cells. Briefly, RLE-6TN cells were seeded into Flexcell culture plates (6-well plates) and subjected to mechanical stresses with varying amplitudes (5%, 10%, and 15%) for different durations (6, 12, and 24 h). The frequency and waveform of the mechanical stretch were set to 0.3 Hz and a sine wave, respectively.

RLE-6TN cells from 10% MS, Lv-NC and Lv-BDKRB1 groups were treated with 10% mechanical stress for 12 h.

Flow cytometry

A cell cycle detection kit (7sea Biotech, China) and Fluo-3 AM probe (Beyotime, China), in combination with flow cytometry, were employed to assess the cell cycle distribution and calcium influx in RLE-6TN cells. For the cell cycle assays, RLE-6TN were incubated with 0.5 mL of propylene iodide (PI) staining solution for 30 min. For the calcium influx assay, RLE-6TN were incubated with 5 μ M Fluo-3 AM for 45 min. After washing, RLE-6TN cells were further incubated for an additional 30 min to ensure the complete hydrolysis of Fluo-3 AM into Fluo-3. The proportion of PI⁺ and Fluo-3⁺ cells were analyzed using a flow cytometer (Novocyte advanceon; Agilent, USA) to evaluate cell cycle distribution and calcium influx.

EDU staining

BeyoClick™ EdU-594 kit (Beyotime) was used to detect RLE-6TN cell proliferation. RLE-6TN cells were cultured in 24-well plates and subsequently incubated for 2 h with 20 μ M 2 \times EDU working solution. EDU-labeled RLE-6TN cells were fixed using 4% paraformaldehyde for 15 min. Cells were washed and permeabilized sequentially with 3% BSA and 0.3% Triton X-100. Cells were incubated for 30 min with 0.5 mL of Click reaction solution and subsequently blocked using antifade mountant with DAPI. A fluorescence microscope (BX53; Olympus, Japan) was used to collect cell images.

Western blotting assay

Total protein was extracted from RLE-6TN cells using RIPA lysis buffer (Sangon, China), and protein concentrations were measured using a BCA assay kit (Thermo Scientific, USA). Equal amounts of protein from each group were mixed with 5 \times loading buffer and denatured in a metal bath (Thermo Scientific) for 10 min. Denatured protein samples were separated by SDS-PAGE and transferred onto PVDF membranes using a vertical Trans-Blot. Membranes were blocked in 5% skimmed milk powder (Beyotime) for 1 h and then incubated in hybridization bags with primary antibodies: rabbit PcAb anti-BDKRB1 (1:2000; Novus Biologicals, USA), rabbit PcAb anti-THBS1 (1:2000; Bioss, China), rabbit PcAb anti-MEK1 (1:2000; Affinity Biosciences, USA), rabbit mcAb anti-p-MEK1 (1:5000; Abcam, USA), rabbit PcAb anti-ERK1/2 (1:5000; Affinity Biosciences), rabbit mcAb anti-p-ERK1/2 (1:1000; Invitrogen, USA), rabbit PcAb anti-CaMKII α / δ (1:2000; Invitrogen), mouse mcAb anti- β -actin (1:4000; ZSGB-BIO, China), goat anti-mouse IgG HRP (1:4000; Abmart, USA), and goat anti-rabbit IgG HRP (1:4000; Abmart). Protein signals were visualized

using an ECL kit (Invitrogen) and captured with a 5200Multi chemiluminescence instrument (Tanon, China).

RNA extraction and RT-qPCR assay

Total RNA was extracted from RLE-6TN cells using the TRIzol™ Plus Kit (Invitrogen), and RNA concentrations were determined using a UV spectrophotometer (EzDrop1000; BLUE-RAY, China). Reverse transcription was performed using the FastKing cDNA Kit (Tiangen, Germany) to synthesize cDNA from the extracted RNA. PCR amplification of target genes was conducted using a 7500 Fluorescent Quantitative PCR System (ABI, USA) and the SYBR qPCR Master Mix Kit (Vazyme, China). β -actin was used as the internal control. The primer sequences used are as follows: CTGGAGAAGAGCTATGAG (β -actin-F), GATGGAATTGAATGTAGTTTC (β -actin-R), AAGGATGGTGGAGTTGAA (BDKRB1-F), CAGGATGTGATAGTTGAAGAA (BDKRB1-R), TGGATTACATCGTCAATGAG (MEK1-F), AGGGTTCTTTATTAAGCACTT (MEK1-R), CCCAAATCTGACTCCAAA (ERK1-F), TGCTTCCTCTACTGTGAT (ERK1-R), TTGTTCTGCTTATGATAATCTC (ERK2-F), ATTGATGCCGATGATGTT (ERK2-R), GCACCACTACCTTATCTT (CaMKII α -F), AGCCTC ACTGTAATACTC (CaMKII α -R), CGTCATCCTCTA CATCTT (CaMKII δ -F), ATCTGCTGATACAGTCTAT (CaMKII δ -R), CAGGAAGACTATGACAAG (THBS1-F), and TAATGGAATGGACAGTTG (THBS1-R).

Statistical analysis

All experiments were performed with a minimum of three biological replicates, and the data were conformed to follow a normal distribution. Statistical analysis and data visualization were conducted using GraphPad Prism software (GraphPad, USA). Error bars in all graphs represent the mean \pm SD. Comparisons between two groups were assessed using Student's t test, while comparisons among multiple groups were conducted using one-way ANOVA. A $p < 0.05$ was considered statistically significant.

Results

Effects of mechanical stress on the viability, cycle, and calcium influx of RLE-6TN cells

This study investigated the effects of mechanical stresses at varying amplitudes (5%, 10%, and 15%) on alveolar epithelial cell growth and calcium homeostasis. CCK-8 assay revealed that a 5% mechanical stress applied for 6, 12, and 24 h did not significantly affect the viability of RLE-6TN cells (Fig. 1A, $P > 0.05$). In contrast, a 10% mechanical stress treatment for 12 and 24 h significantly enhanced cell viability, whereas

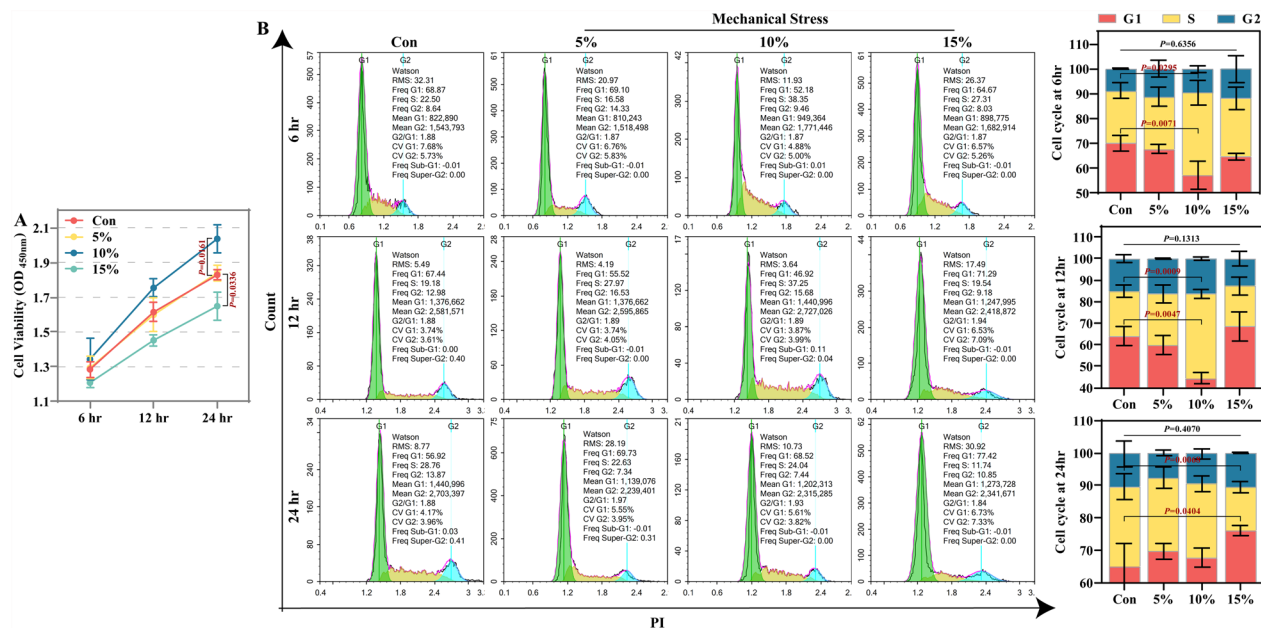


Fig. 1 Effects of mechanical stress on the viability and cycle of RLE-6TN cells. **A** CCK-8 experiments were performed to detect the viability of RLE-6TN cells after different amplitudes (5%, 10% and 15%) of mechanical stress treatment for different times (6 h, 12 h and 24 h). **B** The effects of mechanical stress with different magnitudes (5%, 10% and 15%) on the cycle of RLE-6TN cells were identified using flow cytometry in combination with PI staining. N = 3, one-way ANOVA with Tukey's multiple comparisons test

a 15% stress amplitude significantly reduced viability (Fig. 1A, $P < 0.05$). Flow cytometry analysis showed that mechanical stress at various amplitudes did not significantly impact the proportion of RLE-6TN cells in the G2 phase (Fig. 1B, $P > 0.05$). Furthermore, treatment with 5% amplitudes for 6, 12, and 24 h did not significantly alter the distribution of cells in the G1, S, and G2 phases (Fig. 1B, $P > 0.05$). However, a 10% amplitude for 6 and 12 h led to a reduced proportion of cells in G1 and an increased proportion in the S phase (Fig. 1B, $P < 0.05$). Conversely, treatment with a 15% amplitude for 12 and 24 h resulted in an increase proportion in the G1 phase and a decrease in proportion in the S phase (Fig. 1B, $P < 0.05$). Additionally, the effects of mechanical stress on cell proliferation were evaluated using EdU staining. The 10% mechanical stress significantly increased the EdU-positive ratio at all time points, while the 15% stress significantly decreased it (Fig. 2, $P < 0.05$). These findings suggest that 10% mechanical stress promotes RLE-6TN cell growth, whereas 15% stress inhibits cell proliferation. Notably, mechanical stress treatment for 6 h at any amplitude did not significantly alter the proportion of Fluo-3⁺ cells (Fig. 3, $P > 0.05$). In contrast, treatments at 12 and 24 h significantly increased the proportion of Fluo-3⁺ cells (Fig. 3, $P < 0.05$), indicating

enhanced calcium influx in response to mechanical stress.

Mechanical stress activates the BDKRB1/Ca²⁺/CaMKII/MEK1/ERK axis in RLE-6TN cells

Notably, previous studies have demonstrated that BDKRB1 and CaMKII α/δ are associated with calcium metabolism [19, 23, 24]. Therefore, this study further explored the effects of mechanical stresses at varying amplitudes (5%, 10%, and 15%) on the expression of BDKRB1 and CaMKII α/δ in alveolar epithelial cells. RT-qPCR analysis showed that 5% mechanical stress had no significant effect on the mRNA levels of BDKRB1 and CaMKII α/δ (Fig. 4A, $P > 0.05$). In contrast, 10% and 15% mechanical stress treatments for 6, 12, and 24 h significantly increased the mRNA levels of these genes in RLE-6TN (Fig. 4A, $P < 0.05$). These findings suggest that mechanical stress may induce calcium influx in alveolar epithelial cells by upregulating BDKRB1 and CaMKII α/δ . Notably, calcium metabolism regulates cell growth, which is associated with the MEK1/ERK pathway [25, 26]. Therefore, the present study further observed changes in the activity of MEK1/ERK pathway in RLE-6TN cells. A 15% mechanical stress applied for 12 and 24 h significantly decreased the mRNA levels of MEK1, ERK1, and ERK2 (Fig. 4B, $P < 0.05$), while other amplitudes showed no significant effect (Fig. 4B,

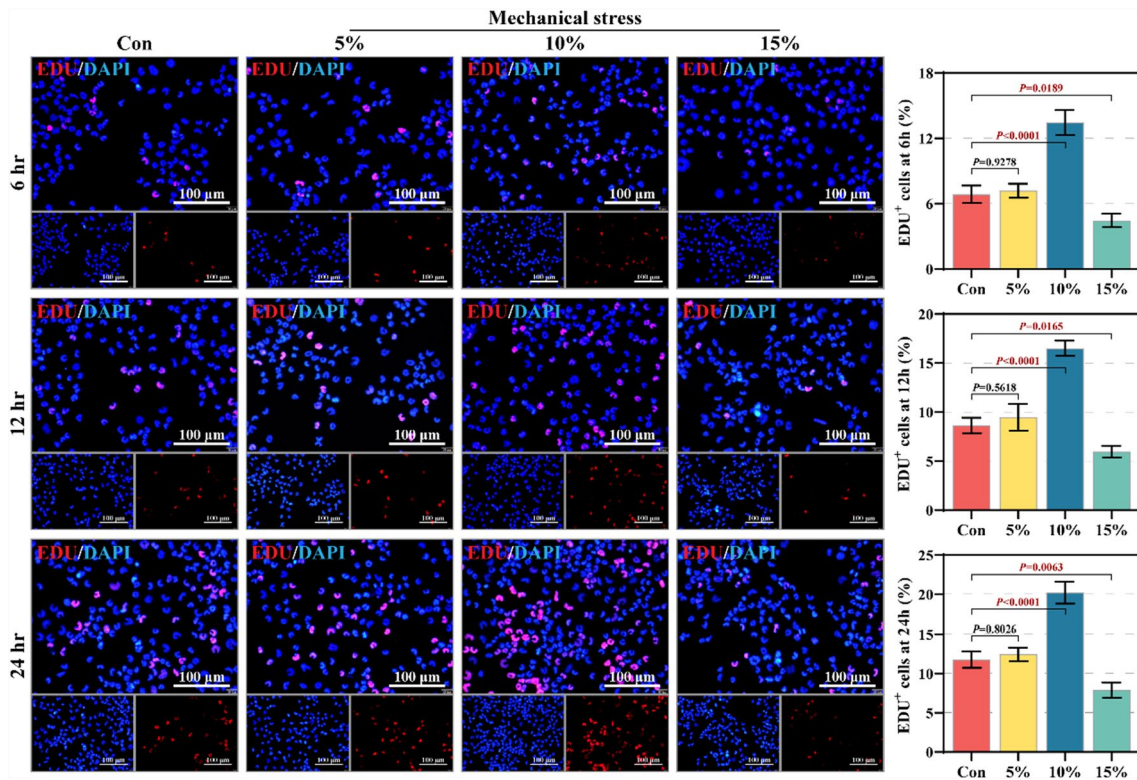


Fig. 2 Effects of mechanical stress on the proliferation of RLE-6TN cells. The proliferation of RLE-6TN cells was detected by EDU staining. Scale: 100µm. N = 3, one-way ANOVA with Tukey's multiple comparisons test

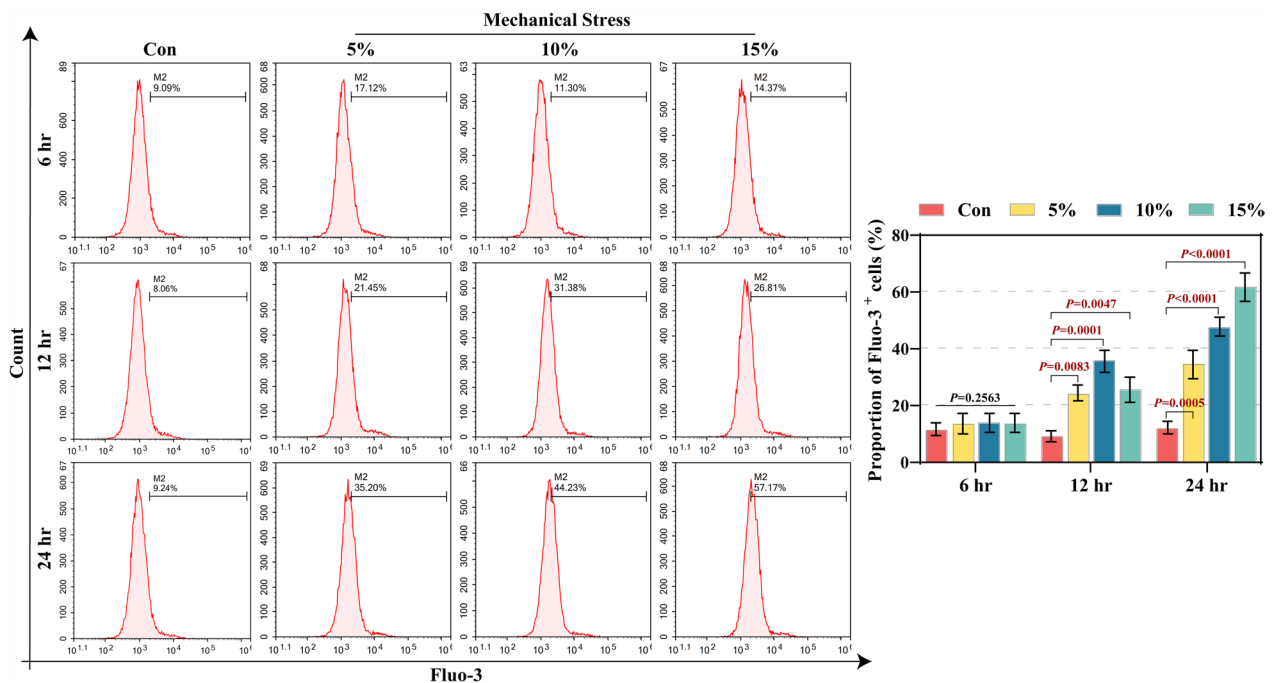


Fig. 3 Effect of mechanical stress on Ca^{2+} concentration in RLE-6TN cells. Ca^{2+} concentration in RLE-6TN cells after mechanical stress treatments with different amplitudes (5%, 10% and 15%) for different times (6 h, 12 h and 24 h) was detected using Fluo-3 AM probe combined with flow cytometry. N = 3, one-way ANOVA with Tukey's multiple comparisons test

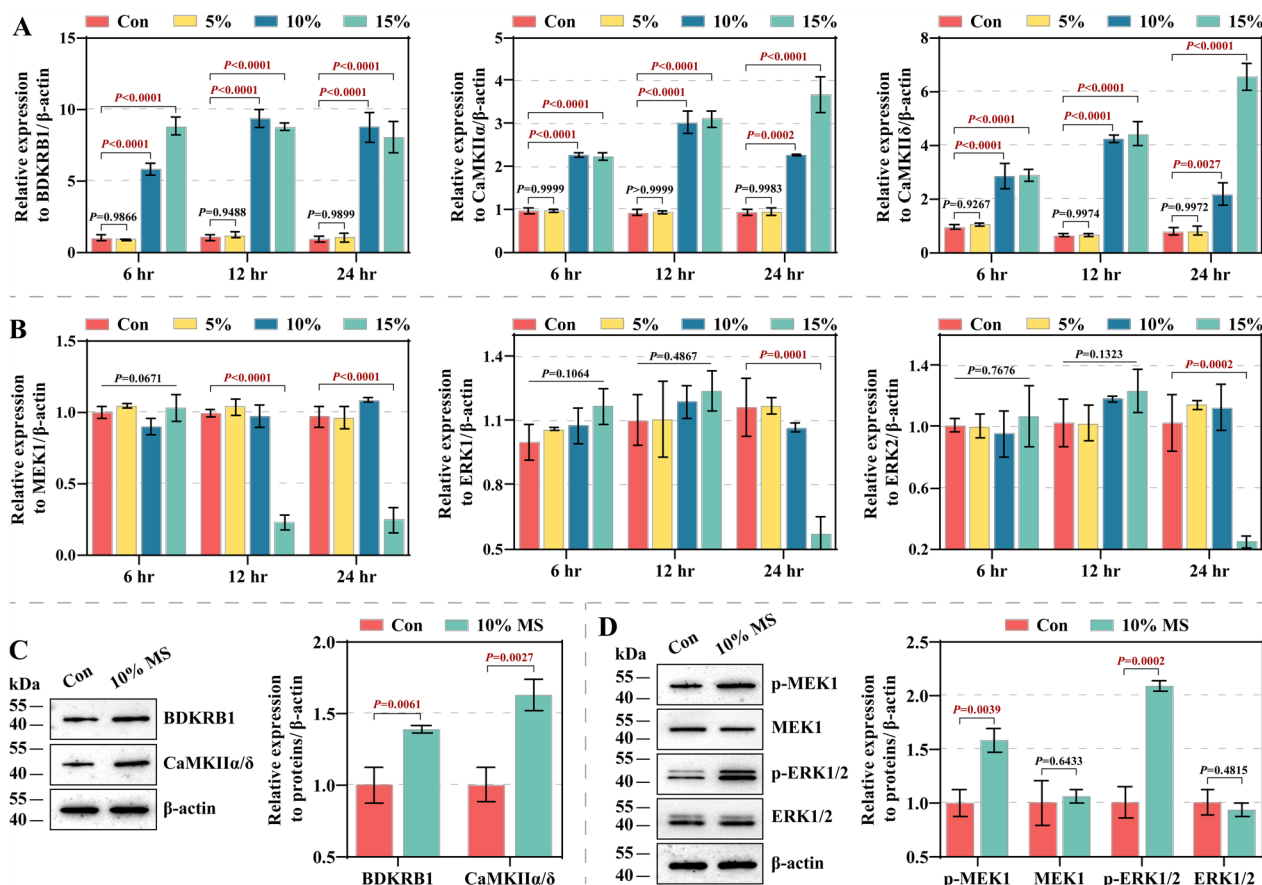


Fig. 4 Effect of mechanical stress on BDKRB1/Ca²⁺/CaMKII/MEK1/ERK axis in RLE-6TN cells. **A, B** RT-qPCR experiments were performed to detect the mRNA levels of BDKRB1/CaMKIIα/δ (**A**) and MEK1/ERK (**B**) in RLE-6TN cells after mechanical stress treatments with different amplitudes (5%, 10%, and 15%) for different times (6 h, 12 h, and 24 h). N=3, one-way ANOVA with Tukey's multiple comparisons tests. **C, D** The effects of mechanical stress with different amplitudes (5%, 10%, and 15%) on the levels of BDKRB1/CaMKIIα/δ (**C**) and MEK1/ERK (**D**) proteins in RLE-6TN cells were examined by Western blotting assay. Complete and uncropped gel imprints are available in the supplementary file. N=3, student's t test

$P > 0.05$). Given that 10% mechanical stress for 12 h promoted both cell growth and calcium influx, its effect on the BDKRB1/Ca²⁺/CaMKII/MEK1/ERK axis was subsequently investigated at the protein level. Western blotting analysis revealed that this condition upregulated the protein levels of BDKRB1, CaMKIIα/δ, p-MEK1, and p-ERK1/2 (Fig. 4C, D, $P < 0.05$). These findings indicate that 10% mechanical stress activates the BDKRB1/Ca²⁺/CaMKII/MEK1/ERK axis, potentially contributing to enhanced growth and calcium influx in RLE-6TN cells.

BDKRB1 knockdown restricts the growth and calcium influx by mechanical stress in RLE-6TN cells

To verify whether the effects of 10% mechanical stress are mediated through the BDKRB1/Ca²⁺/CaMKII/MEK1/ERK axis, this study utilized lentiviral-mediated RNA interference to knock down BDKRB1 expression in RLE-6TN cells. Among the three interfering

lentiviral constructs (#1, #2, and #3), constructs #1 and #3 achieved the most substantial knockdown, reducing BDKRB1 mRNA levels by 80% and 81%, respectively, while construct #2 achieved a 39% reduction (Fig. 5A, $P < 0.05$). Lv-BDKRB1 #3 demonstrated the highest knockdown efficiency and was therefore selected for subsequent experiments. As expected, treatment with 10% mechanical stress effectively enhanced cell viability, the S-phase proportion, EDU positive ratio, and Ca²⁺ concentration compared to the Con group (Fig. 5B–E, $P < 0.05$). Compared with the 10% MS group, the Lv-NC group showed no significant differences in these parameters (Fig. 5B–E, $P < 0.05$). Notably, knockdown of BDKRB1 resulted in 10%, 30%, 30%, and 70% reductions in viability, S-phase proportion, EdU-positive ratio, and Ca²⁺ concentration, respectively, alongside a 22% increase in the G1-phase cell population compared to the Lv-NC group (Fig. 5B–E, $P < 0.05$). These findings indicate that the inhibition

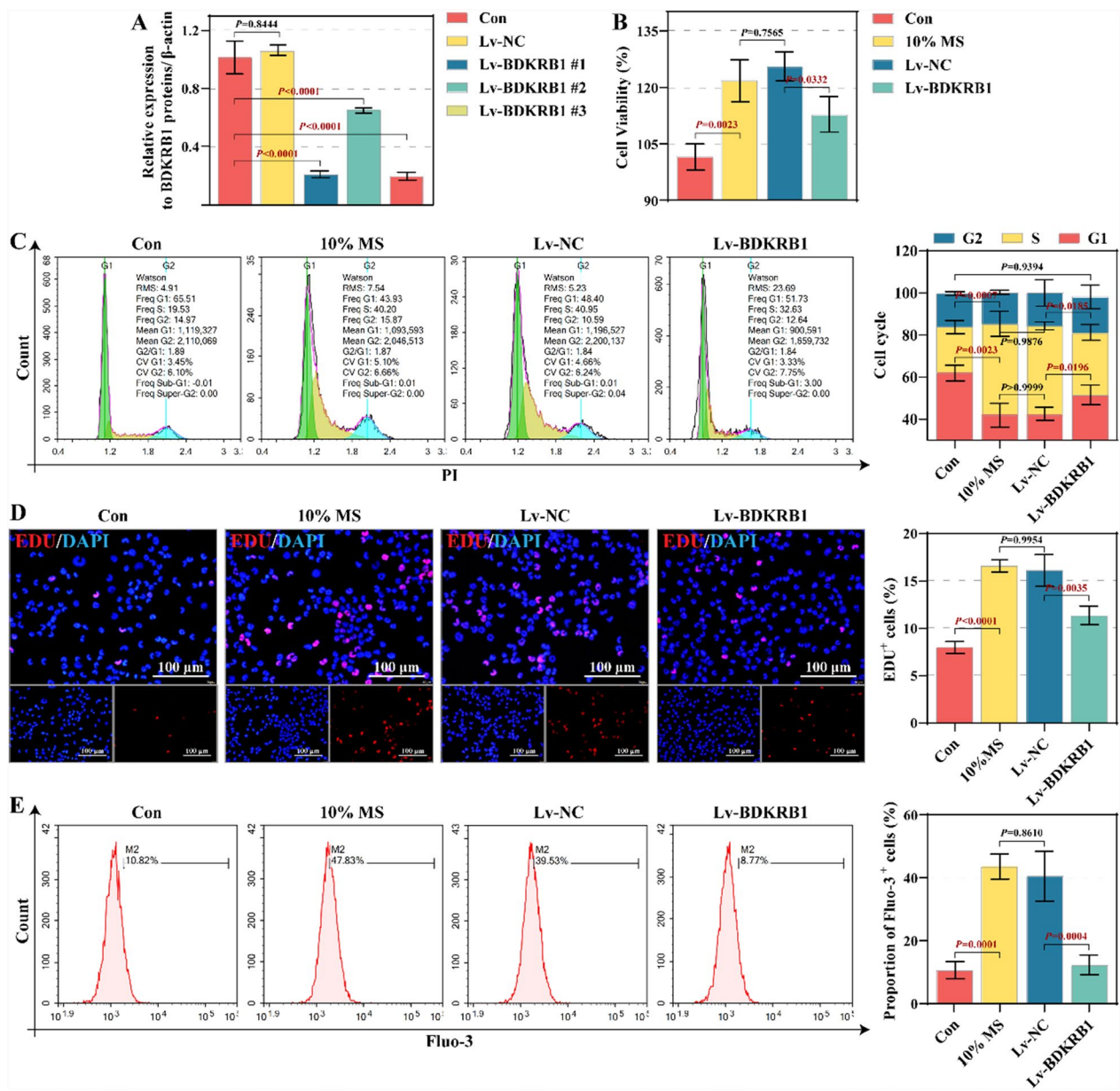


Fig. 5 Effects of BDKRB1 knockdown on mechanical stress-mediated growth and calcium influx in RLE-6TN cells. **A** The effect of BDKRB1 interfering lentivirus and its negative control on BDKRB1 levels in RLE-6TN cells. **B** The effect of BDKRB1 and 10% mechanical stress on the viability of RLE-6TN cells was examined by CCK-8 assay. **C** Flow cytometry combined with PI staining identified the effects of BDKRB1 and 10% mechanical stress on the RLE-6TN cell cycle. **D** Representative picture of EDU staining for RLE-6TN cells. Scale: 100μm. **E** Fluo-3 AM probe combined with flow cytometry was used to detect Ca²⁺ concentration in RLE-6TN cells after treatment with 10% mechanical stress and BDKRB1 interfering lentivirus. RLE-6TN cells in the Con group were subjected to normal culture. RLE-6TN cells in 10% MS group were subjected to 10% mechanical stress treatment for 12 h. RLE-6TN cells in Lv-NC group were subjected to 10% mechanical stress and a negative control of lentivirus. RLE-6TN cells in Lv-BDKRB1 group were subjected to 10% mechanical stress and BDKRB1 interfering lentivirus. N = 3, one-way ANOVA with Tukey's multiple comparisons test

of BDKRB1 attenuates the stimulatory effects of 10% mechanical stress on growth and calcium influx in RLE-6TN cells.

BDKRB1 knockdown constrains the activation of the Ca²⁺/CaMKII/MEK1/ERK axis by mechanical stress in RLE-6TN cells

Further, this study investigated the effect of BDKRB1 inhibition on the 10% mechanical stress-mediated

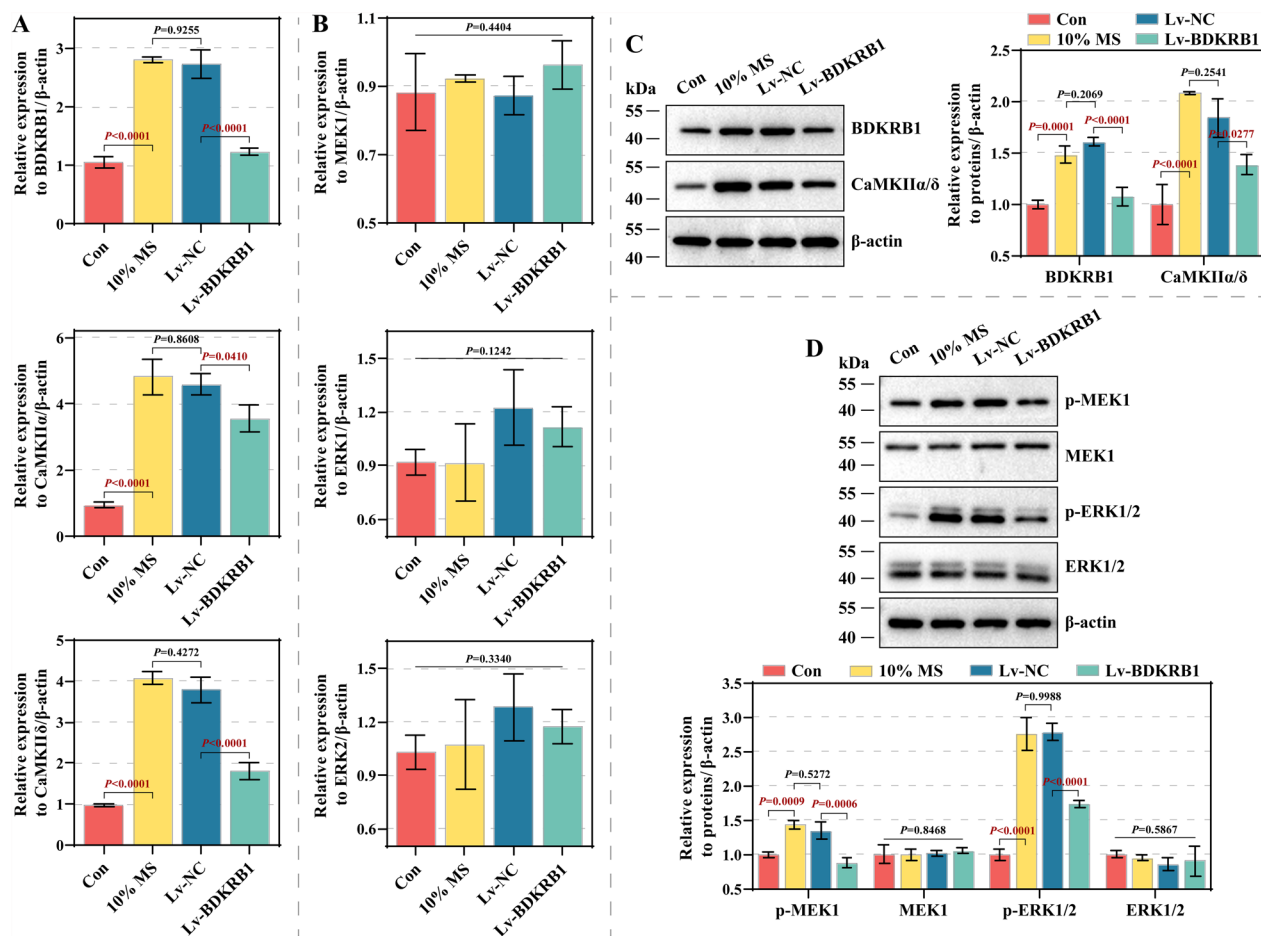


Fig. 6 Effect of BDKRB1 knockdown on mechanical stress-mediated Ca^{2+} /CaMKII/MEK1/ERK axis in RLE-6TN cells. **A, B** The effects of BDKRB1 and 10% mechanical stress on the mRNA levels of BDKRB1/CaMKII α/δ (**A**) and MEK1/ERK (**B**) in RLE-6TN cells were examined by RT-qPCR assay. **C, D** Representative images of gel blot for BDKRB1/CaMKII α/δ (**C**) and MEK1/ERK (**D**), and statistical analysis of the corresponding gray values. Complete and uncropped gel imprints are available in the supplementary file. $N=3$, one-way ANOVA with Tukey's multiple comparisons test

the BDKRB1/ Ca^{2+} /CaMKII/MEK1/ERK axis. Consistent with previous results, 10% mechanical stress significantly increased the levels of BDKRB1, CaMKII α/δ , p-MEK1, and p-ERK1/2 in RLE-6TN cells ($P < 0.05$), without affecting the expression of MEK1 and ERK1/2 mRNA or protein (Fig. 6A–D, $P > 0.05$). Additionally, the negative control (Lv-NC) had no observable effect on the action of 10% mechanical stress (Fig. 6A–D, $P > 0.05$). Notably, BDKRB1 knockdown resulted in 55%, 22%, and 52% reductions in BDKRB1, CaMKII α , and CaMKII δ mRNA levels, respectively, compared to the Lv-NC group (Fig. 6A). Similarly, BDKRB1 and CaMKII α/δ protein levels were reduced by 33% and 25%, respectively (Fig. 6C, $P < 0.05$). Moreover, knockdown of BDKRB1 significantly reduced the levels of p-MEK1 and p-ERK1/2 ($P < 0.05$), while having no significant effect on total MEK1 and ERK1/2 mRNA or protein expression (Fig. 6B

and Fig. 6D, $P > 0.05$). These findings indicate that BDKRB1 inhibition impairs the stimulatory effect of 10% mechanical stress on the Ca^{2+} /CaMKII/MEK1/ERK axis in RLE-6TN cells.

Discussion

This study explored the effects of mechanical stress on the growth and calcium metabolism of alveolar epithelial cells, as well as the underlying molecular mechanisms. Previous studies have shown that mechanical stress in the range of 1%–5% reflects the magnitude of forces experienced by alveolar epithelial cells during normal respiration, whereas 15% mechanical stress simulates the forces generated during moderate tidal volume mechanical ventilation [27]. Therefore, stress amplitudes of 5%, 10%, and 15% were selected to investigate their effects on the growth and calcium influx of RLE-6TN cells. The results showed that 10% mechanical stress facilitated the growth

of RLE-6TN cells, 15% mechanical stress inhibited it, and 5% mechanical stress exerted no significant effect. Previous research has mainly focused on the pro-apoptotic effects of mechanical stress, rather than its influence on cellular proliferation. For example, Ning et al. [28] reported that 5% mechanical stress did not affect apoptosis of A549 cells, whereas 15% induced apoptosis. The current findings are consistent, as 5% mechanical stress did no effect the proliferation of RLE-6TN cells, while 15% mechanical stress reduced proliferation of RLE-6TN cells. Notably, A549 cells share many characteristics with alveolar type II epithelial cells, similar to RLE-6TN cells. Although mechanical stress of 15% or greater has commonly been used to model ventilation-induced lung injury or pulmonary hypertension [29–32], these studies have largely overlooked the effects of sub-threshold stresses. To our knowledge, this is the first study to demonstrate that 10% mechanical stress supports the growth of alveolar epithelial cells. Furthermore, we found that 5%, 10%, and 15% mechanical stresses all facilitated calcium influx in RLE-6TN cells, consistent with previous reports [33, 34]. Interestingly, while both 10% and 15% mechanical stress increased BDKRB1 and CaMKII expression, only 15% stress reduced MEK1 and ERK1/2 expression. This may be due to 15% mechanical stress impairing ERK activity via activation of the p38 MAPK pathway, leading to phosphorylation of MEK1 inhibitory sites or induction of ERK phosphatases (DUSPs) [35, 36]. Additionally, calcium overload induced by 15% stress may activate calcium-dependent apoptotic pathways or mitochondrial dysfunction [37, 38], which may antagonize ERK-mediated signaling. Elevated ROS levels under 15% stress may also contribute to ERK dephosphorylation through oxidation of MEK/ERK or activation of MAPK phosphatases [39]. In conclusion, 15% mechanical stress appears to inhibit MEK/ERK signaling via antagonistic pathway activation, calcium overload, and oxidative stress, ultimately leading to reduced cell viability. In contrast, 10% mechanical stress supports the balance between cell proliferation and calcium homeostasis through activation of the BDKRB1/CaMKII/MEK/ERK axis. These findings highlight the presence of a threshold effect in the biological response to mechanical stress.

The present study further revealed that the effect of 10% mechanical stress on the growth and calcium influx of alveolar epithelial cells is closely associated with BDKRB1. To date, no studies have reported a relationship between BDKRB1 and cell growth, including alveolar epithelial cell. However, BDKRB1 has been linked to calcium metabolism and is known to facilitates Ca^{2+} transport into cell [19, 23, 24]. In this study, 10% mechanical stress increased BDKRB1 expression in RLE-6TN cells, and knockdown of BDKRB1 limited calcium

influx. Thus, BDKRB1 is a cause of calcium influx in RLE-6TN cells induced by 10% mechanical stress. These findings suggest that BDKRB1 mediates calcium influx induced by 10% mechanical stress in RLE-6TN cells. CaMKII is a ubiquitous serine-threonine kinase composed of a monomeric structure that includes an N-terminal catalytic region, a regulatory segment, and a C-terminal association domain [23, 40, 41]. As a key intracellular Ca^{2+} sensor, CaMKII plays a crucial role in Ca^{2+} signaling and can directly transduce the biological effects of elevated Ca^{2+} . Its high affinity for Ca^{2+} /CaM complexes allows it to detect subtle changes in intracellular Ca^{2+} concentration. Under low Ca^{2+} concentrations, CaMKII remains inactive. When intracellular Ca^{2+} levels rise, the Ca^{2+} /CaM complex binds to the regulatory domain of CaMKII, promoting its autophosphorylation and activation. In this study, 10% mechanical stress increased CaMKII α/δ expression in RLE-6TN cells, consistent with the observed calcium influx under the same conditions. Importantly, Ca^{2+} /CaMKII signal can activates the MEK1/ERK pathway, thereby inducing cell growth [42–44]. Our results showed that 10% mechanical stress elevated levels of MEK1 and ERK1/2 phosphorylation, indicating pathway activation. Furthermore, knockdown of BDKRB1 limited activation of the Ca^{2+} /CaMKII/MEK1/ERK signaling pathway by 10% mechanical stress and inhibited RLE-6TN cell growth. This could explain why BDKRB1 can affect the growth of RLE-6TN cells. Notably, excessive ERK1/2 activation and calcium overload may contribute to pulmonary edema by inhibiting the Na^+/K^+ -ATPase [45, 46]. However, the present study found that 10% mechanical stress induced ERK1/2 phosphorylation and calcium influx in a manner that supported cell proliferation, indicating a dose-dependent response. This suggests that moderate mechanical stress may play a critical role in maintaining physiological signaling balance. Specifically, mechanical stress at a physiologic level (e.g., 10%) may promote alveolar repair through activation of the BDKRB1/ Ca^{2+} /CaMKII/MEK1/ERK axis, whereas pathologically high stress (e.g., 15%) may dysregulate this pathway through mechanisms such as oxidative stress or inflammation.

The experimental design of this study focused exclusively on alveolar epithelial cells (RLE-6TN cell line). However, mechanical stress responses may vary significantly among different cell types within lung tissue, such as airway epithelial cells, endothelial cells, and mesenchymal cells. Moreover, this study did not incorporate three-dimensional culture models or in vivo animal models, which could provide additional insights into the role of cell-substrate interactions in modulating mechanical stress responses. Therefore, the current conclusions

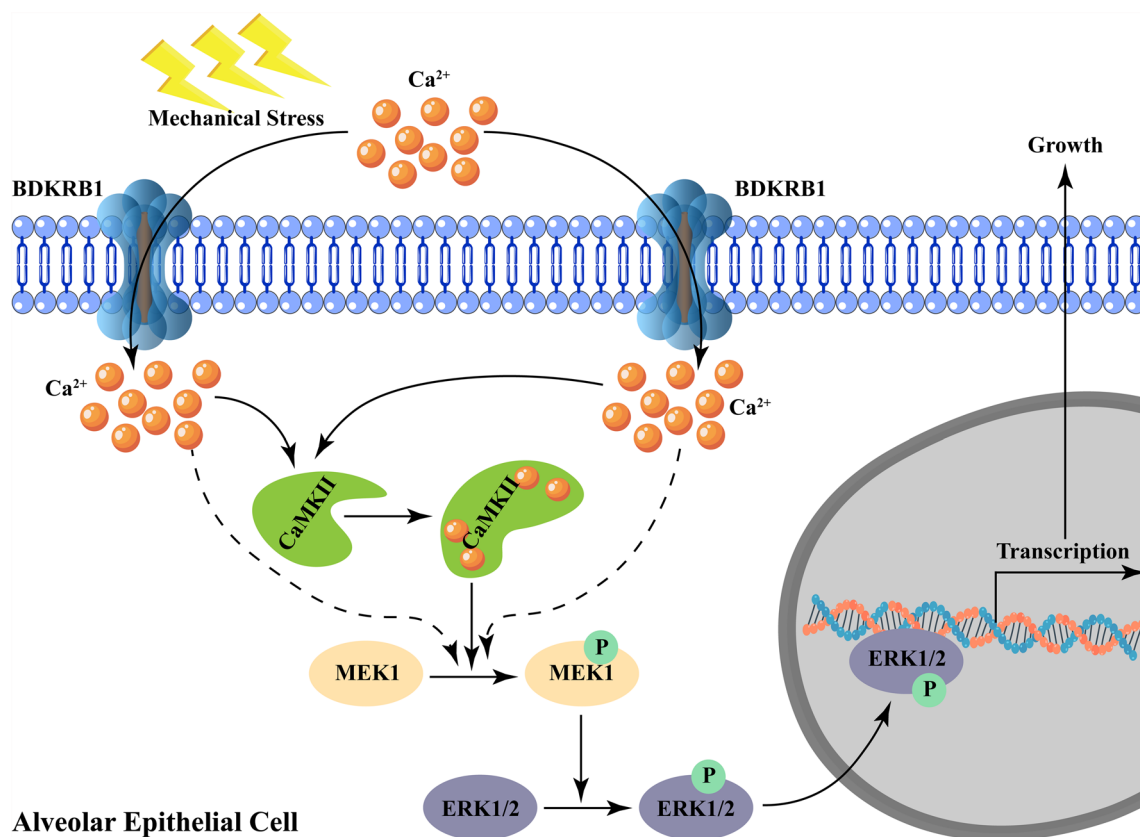


Fig. 7 Mechanical stress-related signaling mechanisms in this study

should be interpreted with caution when extrapolating to other lung cell types or physiological contexts. Future studies should aim to validate the scalability of these findings by integrating primary lung cells, organoid systems, or animal models.

Previous research has demonstrated that mechanosensitive channels such as TRPV4 and Piezo1 contribute to calcium responses in alveolar epithelial cells [29, 47]. While this study focused on the role of BDKRB1, the involvement of other calcium channels under specific mechanical stress conditions warrants further investigation. It is plausible that 10% and 15% mechanical stress modulate calcium homeostasis via distinct combinations of calcium channels. Specifically, BDKRB1 may be the predominant regulator under 10% stress, whereas 15% mechanical stress may induce apoptosis through hyperactivation of TRPV4 and Piezo1 or mitochondrial calcium overload, ultimately reducing cell viability [29, 37, 38, 47]. This hypothesis should be examined in future studies by assessing the expression and activity of TRPV4 and Piezo1 under different mechanical stress amplitudes. Additionally, the use of calcium channel inhibitors will help delineate the contribution of various calcium influx pathways.

CaMKII is known to promote cell proliferation by directly activating the MEK/ERK pathway and upregulating downstream transcription factors [42–44]. Although the present study did not directly assess ERK1/2 downstream targets, changes in cell viability, cell cycle progression, and proliferation collectively reflect the functional relevance of this pathway. Furthermore, the reduction in MEK1 and ERK1/2 phosphorylation following BDKRB1 knockdown reinforces the dependence of this signaling axis. Future investigations should aim to elucidate downstream effector molecules by selectively inhibiting CaMKII or ERK1/2 and examining the expression profiles of related target genes.

In conclusion, this study identified specific mechanical stress conditions and their associated molecular mechanisms that facilitate the growth of RLE-6TN cells. Mechanical stress with 10% amplitude contributes to calcium influx by upregulating BDKRB1 expression, thereby enhancing the growth of RLE-6TN cells through activation of the CaMKII/MEK1/ERK signaling pathway

(Fig. 7). These findings highlight a calcium metabolism-related mechanotransduction mechanism and provide a valuable theoretical framework for understanding and potentially treating mechanical stress-related lung diseases.

Supplementary Information

The online version contains supplementary material available at <https://doi.org/10.1186/s12931-025-03240-7>.

Supplementary Material 1. Original Gel Blot. Complete and uncropped gel blot of western blotting assay.

Author contributions

Conceptualization, Y.Z., and Q.Z.; Performed the experiments, Y.Z., Q.Z., Q.L., Z.S., C.P., R.Y., D.F., S.X., and Y.L.; Analyzed the data, Y.Z. and Q.Z.; resources, Q.L. and Z.S.; Data Curation, Y.Z. and Q.Z.; Writing-original draft preparation, Y.Z. and Q.Z.; Writing-review and editing, Q.L., Z.S., C.P., R.Y., D.F., S.X., and Y.L. All authors have read and agreed to the published version of the manuscript.

Funding

This study was supported by the Project funded by the "Famous Doctor" Special Fund of Yunnan Revitalization Talent Support Program (Zhang Ying in 2022-XDYC-MY-2022-0026), the National Natural Science Foundation of China (82060414), the Special and Joint Program of Yunnan Provincial Science and Technology Department & Kunming Medical University (202101AY070001-150), and the Key Research and Development Program of Yunnan Provincial Science and Technology Department (202403AC100008).

Data availability

All the data obtained and materials analyzed in this research are available with the corresponding author.

Declarations

Ethics approval and consent to participate

Not applicable.

Consent for publication

Not applicable.

Competing interests

The authors declare no competing interests.

Author details

¹Department of Orthopedics, The Second Affiliated Hospital of Kunming Medical University, No.374, Dianmian Avenue, Kunming, Yunnan, China.

²Department of Surgery, Yuxi Hospital Affiliated to Kunming University of Science and Technology, The Second People's Hospital of Yuxi, No.4 Xingyun Road, Yuxi, Yunnan, China.

Received: 21 January 2025 Accepted: 16 April 2025

Published online: 28 April 2025

References

- Long Y, Niu Y, Liang K, Du Y. Mechanical communication in fibrosis progression. *Trends Cell Biol.* 2022;32(1):70–90.
- Lin C, Zheng X, Lin S, Zhang Y, Wu J, Li Y. Mechanotransduction regulates the interplays between alveolar epithelial and vascular endothelial cells in lung. *Front Physiol.* 2022;13: 818394.
- Marchionni A, Tonelli R, Cerri S, Castaniere I, Andrisani D, Gozzi F, Bruzzi G, Manicardi L, Moretti A, Demurtas J, Baroncini S, Andreani A, Cappiello GF, Busani S, Fantini R, Tabbi L, Samarelli AV, Clini E. Pulmonary stretch and lung mechanotransduction: implications for progression in the fibrotic lung. *Int J Mol Sci.* 2021;22(12):6443.
- von Düring S, Parhar KKS, Adhikari NKJ, Urner M, Kim SJ, Munshi L, Liu K, Fan E. Understanding ventilator-induced lung injury: the role of mechanical power. *J Crit Care.* 2024;85: 154902.
- Yang J, Pan X, Wang L, Yu G. Alveolar cells under mechanical stressed niche: critical contributors to pulmonary fibrosis. *Mol Med.* 2020;26(1):95.
- Wang A, Valdez-Jasso D. Cellular mechanosignaling in pulmonary arterial hypertension. *Biophys Rev.* 2021;13(5):747–56.
- Sun Z, Guo SS, Fässler R. Integrin-mediated mechanotransduction. *J Cell Biol.* 2016;215(4):445–56.
- Deng Z, Fear MW, SukChoi Y, Wood FM, Allahham A, Mutsaers SE, Prêlé CM. The extracellular matrix and mechanotransduction in pulmonary fibrosis. *Int J Biochem Cell Biol.* 2020;126:105802.
- Meng Z, Qiu Y, Lin KC, Kumar A, Placone JK, Fang C, Wang KC, Lu S, Pan M, Hong AW, Moroishi T, Luo M, Plouffe SW, Diao Y, Ye Z, Park HW, Wang X, Yu FX, Chien S, Wang CY, Ren B, Engler AJ, Guan KL. RAP2 mediates mechanoresponses of the Hippo pathway. *Nature.* 2018;560(7720):655–60.
- Chai KX, Ni A, Wang D, Ward DC, Chao J, Chao L. Genomic DNA sequence, expression, and chromosomal localization of the human B1 bradykinin receptor gene BDKRB1. *Genomics.* 1996;31(1):51–7.
- Xie H, Lu F, Liu W, Wang E, Wang L, Zhong M. Remimazolam alleviates neuropathic pain via regulating bradykinin receptor B1 and autophagy. *J Pharm Pharmacol.* 2021;73(12):1643–51.
- Schulze-Topphoff U, Prat A, Prozorovski T, Siffrin V, Paterka M, Herz J, Bendix I, Ifergan I, Schadock I, Mori MA, Van Horssen J, Schröter F, Smorodchenko A, Han MH, Bader M, Steinman L, Aktas O, Zipp F. Activation of kinin receptor B1 limits encephalitogenic T lymphocyte recruitment to the central nervous system. *Nat Med.* 2009;15(7):788–93.
- Zhang Y, Li Q, Shi Z, Li Q, Dai X, Pan C, Ma Y, Yan R, Fei D, Xie J. A novel growth-friendly system alleviates pulmonary dysplasia in early-onset scoliosis combined with thoracic insufficiency syndrome: radiological, pathological, and transcriptomic assessments. *Heliyon.* 2024;10(6): e27887.
- Kuo IY, Jen J, Hsu LH, Hsu HS, Lai WW, Wang YC. A prognostic predictor panel with DNA methylation biomarkers for early-stage lung adenocarcinoma in Asian and Caucasian populations. *J Biomed Sci.* 2016;23(1):58.
- Emblom-Callahan MC, Chhina MK, Shlobin OA, Ahmad S, Reese ES, Iyer EP, Cox DN, Brenner R, Burton NA, Grant GM, Nathan SD. Genomic phenotype of non-cultured pulmonary fibroblasts in idiopathic pulmonary fibrosis. *Genomics.* 2010;96(3):134–45.
- Ren J, Deng G, Li R, Jin X, Liu J, Li J, Gao Y, Zhang J, Wang X, Wang G. Possible pharmacological targets and mechanisms of sivelestat in protecting acute lung injury. *Comput Biol Med.* 2024;170: 108080.
- Tsukagoshi H, Shimizu Y, Horie T, Fukabori Y, Shimizu Y, Iwamae S, Hisada T, Ishizuka T, Iizuka K, Dobashi K, Mori M. Regulation by interleukin-1beta of gene expression of bradykinin B1 receptor in MH-S murine alveolar macrophage cell line. *Biochem Biophys Res Commun.* 1999;259(2):476–82.
- Gonçalves-Zillo TO, Pugliese LS, Sales VM, Mori MA, Squaiella-Baptistão CC, Longo-Maugéri IM, Lopes JD, de Oliveira SM, Monteiro AC, Pesquero JB. Increased bone loss and amount of osteoclasts in kinin B1 receptor knockout mice. *J Clin Periodontol.* 2013;40(7):653–60.
- Sun DP, Lee YW, Chen JT, Lin YW, Chen RM. The bradykinin-BDKRB1 axis regulates aquaporin 4 gene expression and consequential migration and invasion of malignant glioblastoma cells via a Ca(2+)-MEK1-ERK1/2-NF-κB mechanism. *Cancers.* 2020;12(3):667.
- Murata N, Ito S, Furuya K, Takahara N, Naruse K, Aso H, Kondo M, Sokabe M, Hasegawa Y. Ca²⁺ influx and ATP release mediated by mechanical stretch in human lung fibroblasts. *Biochem Biophys Res Commun.* 2014;453(1):101–5.
- Chatterjee S, Nieman GF, Christie JD, Fisher AB. Shear stress-related mechanosignaling with lung ischemia: lessons from basic research can inform lung transplantation. *Am J Physiol Lung Cell Mol Physiol.* 2014;307(9):L668–80.
- Alevriadou BR, Shanmughapriya S, Patel A, Stathopoulos PB, Madesh M. Mitochondrial Ca(2+) transport in the endothelium: regulation by ions, redox signalling and mechanical forces. *J Royal Soc Interface.* 2017;14(137):20170672.

23. Yasuda R, Hayashi Y, Hell JW. CaMKII: a central molecular organizer of synaptic plasticity, learning and memory. *Nat Rev Neurosci*. 2022;23(11):666–82.
24. Bhattacharyya M, Karandur D, Kuriyan J. Structural insights into the regulation of Ca(2+)/calmodulin-dependent protein kinase II (CaMKII). *Cold Spring Harbor Perspect Biol*. 2020;12(6):a035147.
25. Patergnani S, Danese A, Bouhamida E, Aguiari G, Previati M, Pinton P, Giorgi C. Various aspects of calcium signaling in the regulation of apoptosis, autophagy, cell proliferation, and cancer. *Int J Mol Sci*. 2020;21(21):8323.
26. Rosen LB, Ginty DD, Weber MJ, Greenberg ME. Membrane depolarization and calcium influx stimulate MEK and MAP kinase via activation of Ras. *Neuron*. 1994;12(6):1207–21.
27. Chandel NS, Sznajder JI. Stretching the lung and programmed cell death. *Am J Physiol Lung Cell Mol Physiol*. 2000;279(6):L1003–4.
28. Ning QM, Sun XN, Zhao XK. Role of mechanical stretching and lipopolysaccharide in early apoptosis and IL-8 of alveolar epithelial type II cells A549. *Asian Pac J Trop Med*. 2012;5(8):638–44.
29. Liang GP, Xu J, Cao LL, Zeng YH, Chen BX, Yang J, Zhang ZW, Kang Y. Piezo1 induced apoptosis of type II pneumocytes during ARDS. *Respir Res*. 2019;20(1):118.
30. Raaz U, Kuhn H, Wirtz H, Hammerschmidt S. Rapamycin reduces high-amplitude, mechanical stretch-induced apoptosis in pulmonary microvascular endothelial cells. *Microvasc Res*. 2009;77(3):297–303.
31. Upadhyay D, Correa-Meyer E, Sznajder JI, Kamp DW. FGF-10 prevents mechanical stretch-induced alveolar epithelial cell DNA damage via MAPK activation. *Am J Physiol Lung Cell Mol Physiol*. 2003;284(2):L350–9.
32. Valentine MS, Link PA, Herbert JA, KamgaGnizeko FJ, Schneck MB, Shankar K, Nkwocha J, Reynolds AM, Heise RL. Inflammation and monocyte recruitment due to aging and mechanical stretch in alveolar epithelium are inhibited by the molecular chaperone 4-phenylbutyrate. *Cell Mol Bioeng*. 2018;11(6):495–508.
33. Wirtz HR, Dobbs LG. Calcium mobilization and exocytosis after one mechanical stretch of lung epithelial cells. *Science*. 1990;250(4985):1266–9.
34. Isakson BE, Evans WH, Boitano S. Intercellular Ca²⁺ signaling in alveolar epithelial cells through gap junctions and by extracellular ATP. *Am J Physiol Lung Cell Mol Physiol*. 2001;280(2):L221–8.
35. Seternes OM, Kidger AM, Keyse SM. Dual-specificity MAP kinase phosphatases in health and disease. *Biochimica et biophysica acta. Molecular cell research*. 2019;1866(1):124–43.
36. Cuadrado A, Nebreda AR. Mechanisms and functions of p38 MAPK signalling. *Biochem J*. 2010;429(3):403–17.
37. Moon DO. Calcium's role in orchestrating cancer apoptosis: mitochondrial-centric perspective. *Int J Mol Sci*. 2023;24(10):8982.
38. B. Cartes-Saavedra, A. Ghosh, G. Hajnóczky, The roles of mitochondria in global and local intracellular calcium signalling, *Nat Rev*. 2025.
39. Jomova K, Raptova R, Alomar SY, Alwasel SH, Nepovimova E, Kuca K, Valko M. Reactive oxygen species, toxicity, oxidative stress, and antioxidants: chronic diseases and aging. *Arch Toxicol*. 2023;97(10):2499–574.
40. Nicoll RA, Schulman H. Synaptic memory and CaMKII. *Physiol Rev*. 2023;103(4):2877–925.
41. Reyes Gaido OE, Nkashama LJ, Schole KL, Wang Q, Umapathi P, Mesubi OO, Konstantinidis K, Luczak ED, Anderson ME. CaMKII as a therapeutic target in cardiovascular disease. *Ann Rev Pharmacol Toxicol*. 2023;63:249–72.
42. Lv D, Lin Z, Liao X, Peng R, Liu H, Wu T, Wu K, Sun Y, Zhang Z. Sfrp2 promotes renal dysfunction of diabetic kidney disease via modulating Fzd5-induced cytosolic calcium ion concentration and CaMKII/Mek/Erk pathway in mesangial cells. *Biochim Biophys Acta*. 2024;1870(2): 166933.
43. Illario M, Cavallo AL, Monaco S, Di Vito E, Mueller F, Marzano LA, Troncone G, Fenzi G, Rossi G, Vitale M. Fibronectin-induced proliferation in thyroid cells is mediated by alpha5beta3 integrin through Ras/Raf-1/MEK/ERK and calcium/CaMKII signals. *J Clin Endocrinol Metab*. 2005;90(5):2865–73.
44. Liang D, Zeng Q, Xu Z, Zhang H, Gui L, Xu C, Chen S, Zhang S, Huang S, Chen L. BAFF activates Erk1/2 promoting cell proliferation and survival by Ca²⁺-CaMKII-dependent inhibition of PP2A in normal and neoplastic B-lymphoid cells. *Biochem Pharmacol*. 2014;87(2):332–43.
45. Simonsen U, Wandall-Frostholm C, Oliván-Viguera A, Köhler R. Emerging roles of calcium-activated K channels and TRPV4 channels in lung oedema and pulmonary circulatory collapse. *Acta Physiol (Oxf)*. 2017;219(1):176–87.
46. Wang HC, Zentner MD, Deng HT, Kim KJ, Wu R, Yang PC, Ann DK. Oxidative stress disrupts glucocorticoid hormone-dependent transcription of the amiloride-sensitive epithelial sodium channel alpha-subunit in lung epithelial cells through ERK-dependent and thioredoxin-sensitive pathways. *J Biol Chem*. 2000;275(12):8600–9.
47. Schaller L, Gudermand T, Dietrich A. TRPV4 mediates alveolar epithelial barrier integrity and induces ADAM10-driven E-cadherin shedding. *Cells*. 2024;13(20):1717.

Publisher's Note

Springer Nature remains neutral with regard to jurisdictional claims in published maps and institutional affiliations.